Earth Syst. Sci. Data, 7, 157–171, 2015
www.earth-syst-sci-data.net/7/157/2015/
doi:10.5194/essd-7-157-2015

Open Access Earth System Science Data

Filling the gaps in meteorological continuous data measured at FLUXNET sites with ERA-Interim reanalysis

N. Vuichard[1] **and D. Papale**[2,3]

[1]Laboratoire des Sciences du Climat et de l'Environnement, LSCE/IPSL – UMR CEA/CNRS/UVSQ 8212 CEA Saclay, Orme des Merisiers, Bât 712, 91191 Gif-sur-Yvette, France
[2]Department for Innovation in Biological, Agro-food and Forest systems (DIBAF), University of Tuscia, Viterbo, Italy
[3]Euro-Mediterranean Center on Climate Change (CMCC), Via Augusto Imperatore 16, 73100 Lecce, Italy

Correspondence to: N. Vuichard (vuichard@lsce.ipsl.fr)

Received: 28 November 2014 – Published in Earth Syst. Sci. Data Discuss.: 20 January 2015
Revised: 22 June 2015 – Accepted: 23 June 2015 – Published: 13 July 2015

Abstract. Exchanges of carbon, water and energy between the land surface and the atmosphere are monitored by eddy covariance technique at the ecosystem level. Currently, the FLUXNET database contains more than 500 registered sites, and up to 250 of them share data (free fair-use data set). Many modelling groups use the FLUXNET data set for evaluating ecosystem models' performance, but this requires uninterrupted time series for the meteorological variables used as input. Because original in situ data often contain gaps, from very short (few hours) up to relatively long (some months) ones, we develop a new and robust method for filling the gaps in meteorological data measured at site level. Our approach has the benefit of making use of continuous data available globally (ERA-Interim) and a high temporal resolution spanning from 1989 to today. These data are, however, not measured at site level, and for this reason a method to downscale and correct the ERA-Interim data is needed. We apply this method to the level 4 data (L4) from the La Thuile collection, freely available after registration under a fair-use policy. The performance of the developed method varies across sites and is also function of the meteorological variable. On average over all sites, applying the bias correction method to the ERA-Interim data reduced the mismatch with the in situ data by 10 to 36%, depending on the meteorological variable considered. In comparison to the internal variability of the in situ data, the root mean square error (RMSE) between the in situ data and the unbiased ERA-I (ERA-Interim) data remains relatively large (on average over all sites, from 27 to 76 % of the standard deviation of in situ data, depending on the meteorological variable considered). The performance of the method remains poor for the wind speed field, in particular regarding its capacity to conserve a standard deviation similar to the one measured at FLUXNET stations.

The ERA-Interim reanalysis data de-biased at FLUXNET sites can be downloaded from the PANGAEA data centre (http://doi.pangaea.de/10.1594/PANGAEA.838234).

1 Introduction

In the late 1970s and early 1980s, exchanges of carbon, water and energy between the land surface and the atmosphere began to be monitored by the eddy covariance technique at the ecosystem level (Desjardins and Lemon, 1974; Anderson et al., 1984; Anderson and Verma, 1986; Ohtaki, 1984; Desjardins et al., 1984; Baldocchi, 2003, for a review). Since this period, several networks of eddy sites have been built, on regional or continental scales: Euroflux in 1996 for Europe (Aubinet et al., 2000; Valentini et al., 2000), AmeriFlux in 1997 for North America (Running et al., 1999), AsiaFlux in 1999 for Asia (Kim et al., 2009) and OzFlux in early 2000 for Australia. Currently most of these networks evolved in long-term research infrastructures, such as Integrated Carbon Observation System (ICOS) (www.icos-infrastrucutre.eu), National Ecological Observatory Network (NEON) (www.neoninc.org) and AmeriFlux (http://ameriflux.lbl.gov/). On the global scale, the FLUXNET project that combines these regional and continental networks into an integrated global network started in 1998 (Baldocchi et al., 2001). Currently, the FLUXNET database contains more than 500 registered sites, and up to 250 of them share data (more info on http://www.fluxdata.org). As stated in Baldocchi et al. (2001), the three main scientific goals of the FLUXNET project are

1. to quantify the spatial differences in carbon dioxide and water vapour exchange rates that may be experienced within and across natural ecosystems and climatic gradients;

2. to quantify the temporal dynamics and variability of carbon, water and energy flux densities; and

3. to quantify the variations in carbon dioxide and water vapour fluxes due to changes in insolation, temperature, soil moisture, photosynthetic capacity, nutrition, canopy structure and ecosystem functional type.

These scientific goals have been largely achieved by several publications; examples of other studies published in the last years are Jung et al. (2010), Teuling et al. (2010), Beer et al. (2010), Stoy et al. (2009) and Mahecha et al. (2010).

Many modelling groups have also used the FLUXNET data set for evaluating models' performance at simulating energy, water and carbon exchanges between the surface and the atmosphere. Krinner et al. (2005) evaluate the temporal dynamics (mainly the mean diurnal cycle) of the sensible heat, latent heat, net ecosystem exchange (NEE) and net radiation simulated by the Organising Carbon and Hydrology In Dynamic Ecosystems (ORCHIDEE) model against ~ 30 flux sites across the globe. The community land model (CLM) has been evaluated at 15 FLUXNET sites focusing mainly at the seasonal variability of the latent and sensible heat, the NEE and the GPP (gross primary productivity) (Stöckli et al., 2008). They also make use of the evaluation against FLUXNET data as a way of benchmarking several versions of the CLM model. Similarly, Boussetta et al. (2013) use 35 FLUXNET sites for evaluating and benchmarking the Carbon Tiled ECMWF Scheme for Surface Exchanges over Land (CTESSEL) and Carbon Hydrology Tiled ECMWF Scheme for Surface Exchanges over Land (CHTESSEL) models, looking at the seasonal cycle of the latent and sensible heat, of the NEE and of its components (GPP and total ecosystem respiration (TER)), an analysis extended also to other models by Balzarolo et al. (2014), who looked also at the functional relationships (e.g. GPP–radiation or respiration–temperature) in the data and in the models. Blyth et al. (2010) focus on the evaluation of the evapotranspiration simulated by the Joint UK Land Environment Simulator (JULES) model against 10 FLUXNET sites on annual, seasonal, weekly and diurnal timescales.

In most of these studies, where models are evaluated against in situ FLUXNET data, the attempt is to assess the intrinsic performance of the models and to diagnose a model's parameterization errors or missing processes in the models. Consequently, one wants to make use of meteorological data measured at the FLUXNET sites, jointly with the flux data, to force the models in such a way that errors due to inaccurate meteorological forcing data are avoided. To complement this aim, other studies such as Zhao et al. (2012) examine how errors in meteorological variables impact simulated ecosystem fluxes at FLUXNET sites by using several reanalysis (SAFRAN (Système d'Analyse Fournissant des Renseignements Atmosphériques à la Neige), REMO (Regional Model), ERA-Interim) and in situ data sets.

While models require uninterrupted time series for the meteorological variables used as input, original in situ data often contain gaps, from very short (few hours) up to relatively long (some months) ones. The reasons why meteorological data are missing are few compared to those for flux data (Baldocchi et al., 2001). In the case of meteorological data, gaps are mainly due to calibration and maintenance operations or system breakdown, in particular in remote sites powered by solar panels. These gaps prevent the use of original in situ meteorological data directly as inputs to the models. A gapfilling procedure using adequate methods is consequently needed.

In some of studies, simple gapfilling methods have been developed. For instance, in Blyth et al. (2010), "gap filling involved, for each precise time step that was missing, using the average of values from other years at the same time step". In Stöckli et al. (2008), "up to two month long successive gaps were filled by applying a 30 day running mean diurnal cycle forwards and backwards through the yearly time series. Years with more than 2 month of consecutive missing data were not used".

For long gaps, these simple methods may have strong limitations. Even if the evaluation of the modelled fluxes is only performed when in situ meteorological data are available, for some processes accounting for lag effects, periods where no in situ meteorological data are available may have an important impact on modelled fluxes over later periods, when meteorological data are available.

Other studies develop more sophisticated gapfilling procedures. For example methods, such as artificial neural networks or look-up tables, that are based on the relations between variables, such as the one presented in Papale (2012), and that are generally applied to fill gaps in the fluxes can be successfully used also for gaps in meteorological data. The problem is, however, that often during gap periods in meteorological data, all the variables are missing and so these methods cannot be applied. Krinner et al. (2005) used the ECMWF ERA15 1×1 degree reanalysis for gapfilling the incoming short-wave radiation and weather stations nearby the FLUXNET sites for the other meteorological fields needed for running the ORCHIDEE model.

The main limitations of these more sophisticated gapfilling methods are the lack of tools for evaluating their performances and a non-standardized application.

To overcome these limitations, we develop a new, robust and powerful method, making use of the ERA-Interim reanalysis for filling the gaps in meteorological data measured at FLUXNET sites. This approach has the benefit of making use of continuous data available globally (ERA-Interim) and a high temporal resolution spanning from 1989 to today. The ERA-Interim reanalysis performs well in simulating most of the atmospheric variables that are used for the gapfilling method presented here (Dee et al., 2011), but precipitation is overestimated in tropical areas (Dee et al., 2011; Balsamo et al., 2015) compared to observation-based estimates of the GPCP (Global Precipitation Climatology Project; Adler et al., 2003). Zhao et al. (2012) and Balzarolo et al. (2014) have shown that using raw ERA-Interim data instead of local atmospheric observations has little or no impact on the scores of the simulations of a land surface model with respect to local observations of CO_2 and energy fluxes. However, the good performance is partly explained by the fact that internal model errors may compensate for the errors contained in the ERA-Interim data (Zhao et al., 2012). Beyond the quality of the simulated fluxes, the most important thing is to use data for the gapfilling method that are consistent with the original in situ data. In this respect, diagnosed bias against in situ data should be removed. For this reason a method to downscale and correct the ERA-Interim data is needed. The overall objective of the present paper is to describe in detail the method and tools used to fill the gaps and evaluate the results, estimating error and uncertainty in the gapfilled data.

We first present the data sets used (the FLUXNET data set and the ERA-Interim reanalysis) and the methods developed for filling the gaps. We then present the results of our gapfilling procedure for the overall fair-use data set of FLUXNET sites and discuss the potential use of this method for the ecosystem modelling community and its main limitations.

2 Methods

2.1 FLUXNET data set

We use level 4 data (L4) from the La Thuile collection (http://www.fluxdata.org), based on a fair-use policy, as available in August 2013 (153 sites). Half-hourly values of air temperature (*Ta_f*; °C), global radiation (*Rg_f*; $\mathrm{W\,m^{-2}}$), vapour pressure deficit (*VPD_f*; hPa), wind horizontal speed (*WS_f*; $\mathrm{m\,s^{-1}}$), precipitation (*Precip_f*; $\mathrm{mm\,timestep^{-1}}$) and incoming longwave radiation (*LWin*; $\mathrm{W\,m^{-2}}$) are the six meteorological variables that will be gapfilled. These data were quality controlled and then gapfilled using a look-up table. For this reason we selected only original measured data ($qc = 0$), setting all the other half-hours ($qc > 0$) as missing values.

FLUXNET data are given in Coordinated Universal Time (UTC). The time (z, expressed in relation to UTC) of many FLUXNET sites can be found at http://www.fluxdata.org/DataInfo/Dataset20Doc20Lib/CommonAnc.aspx. At the same address, coordinates (latitude and longitude) of each site are also available.

The variables are classified into two main groups:

1. instantaneous: this group includes air temperature, vapour pressure deficit and wind speed, which are state variables where the instantaneous measurement is relevant as is;

2. averaged: includes the radiation and the precipitation where the relevant value is a flux measured over a time range.

Timestamps in the data indicate the time of measurement in the case of "instantaneous" variables, and in the case of "averaged" variables, the end of the averaging period, which is, in general, 30 min (i.e. first data in the year are for 01 January; 00:30 for the instantaneous variables and for 01 January; 00:00–00:30 for the averaged variables).

2.2 ERA-Interim reanalysis

The ERA-Interim (ERA-I) is the latest reanalysis (Dee et al., 2011) from the European Centre for Medium-range Weather Forecast (ECMWF). It is available from 1989 to the present, on a regular grid (0.7°), at a 3-hourly time resolution. In such a reanalysis, time is expressed in UTC + 0 over all the globe. The ERA-I variables that we use are the temperature at 2 m (*t2m*, K), the surface solar radiation downwards (*Sw*; $\mathrm{W\,m^{-2}}$), the dew point temperature at 2 m (*dt2m*; K), the U and V components of the wind speed at 10 m (*u10* and *v10*; $\mathrm{m\,s^{-1}}$), the total precipitation (*Pr*; metres of water per time step) and the surface thermal radiation downwards (*Lw*; $\mathrm{W\,m^{-2}}$). Similarly to the FLUXNET data set, the timestamp indicates the time of the instantaneous measurement or the end of the averaging period for the averaged variables (i.e. first data in the year are for 01 January; 03:00 for the instantaneous variables and for 01 January; 00:00–03:00 for the averaged variables).

2.3 Gapfilling procedure

2.3.1 Harmonizing variables' units

We first change the units of some ERA-I variables to agree with FLUXNET units: *t2m* from K to °C and *Pr* from m to mm. A vapour pressure deficit inferred from *dt2m* and *t2m*, labelled *VPD_erai* (hPa), is also calculated for comparison with *VPD_f* such that

$$VPD\_erai = e_{\mathrm{sat}} - e, \tag{1}$$

with e (hPa) being the vapour pressure and e_{sat} (hPa) the saturation vapour pressure.

The Magnus–Tetens relationship (Murray, 1967) is used to calculate e and e_{sat}:

$$e = a \exp\left(\frac{b \times dt2m}{dt2m - c}\right) \tag{2}$$

and

$$e_{\mathrm{sat}} = a \exp\left(\frac{b \times t2m}{t2m - c}\right), \tag{3}$$

with *dt2m* and *t2m* expressed in °C and a, b and c being three constants ($a = 6.11 \times 10^{-2}$; $b = 21.874$ if $t2m < 0$ else 17.269; $c = 265.49$ if $t2m < 0$ else 237.29).

2.3.2 Harmonizing variables' time periods

In order to compare ERA-I and FLUXNET data at similar time steps, original FLUXNET meteorological variables, denoted by F, are re-indexed from the FLUXNET (half-hourly resolution) to the ERA-I (3-hourly resolution) time grid, taking into consideration differences in time zone.

For the instantaneous fields (*Ta_f*, *VPD_f*, and *WS_f*), the re-indexed variable denoted F_{E} is defined by the following pseudo-algorithm (Alg. 1).

Algorithm 1

for $j = 1 : n_{\mathrm{E}}$
{
$\quad F_{\mathrm{E},j} = F_{(j r_{\mathrm{E}} + z)/r_{\mathrm{F}}}$
}

where nE (n_{F}) is the length expressed in the number of values of the ERA-I (FLUXNET) time series, r_{E} (r_{F}) the time resolution expressed in hours of the ERA-I (FLUXNET) time series and z the difference in local time from UTC.

When F_j is not defined ($j < 1$ or $j > n_{\mathrm{F}}$), the associated $F_{\mathrm{E},j}$ variable is set to -9999 as a missing value.

Appendix A gives an application of each pseudo-algorithm defined in this paper for a site located in time zone UTC + 2.

For the averaged fields (*Rg_f*, *Precip_f* and *LWin*), the re-indexed variable is defined by Alg. (2).

Algorithm 2

for $j = 1 : n_{\mathrm{E}}$
{
$\quad F_{\mathrm{cum}} = 0$
$\quad$ for $k = (((j-1) r_{\mathrm{E}} + z)/r_{\mathrm{F}} + 1) : ((j r_{\mathrm{E}} + z)/r_F)$
$\quad$ {
$\quad\quad F_{\mathrm{cum}} += F_k$
$\quad$ }
$\quad F_{\mathrm{E},j} = \frac{F_{\mathrm{cum}}}{r_{\mathrm{E}}/r_{\mathrm{F}}}$
}

When an element F_k is not defined ($k < 1$ or $k > n_{\mathrm{F}}$) or is defined as missing value (-9999), the associated $F_{\mathrm{E},j}$ variable is set to -9999 as a missing value.

2.3.3 De-biasing the ERA-I data

We denote the original ERA-I meteorological data by E. In order to correct for the observed bias between E and F_{E}, the slope (s) and the intercept (i) of the linear regression of F_{E} against E are used. The de-biased ERA-I meteorological data is denoted E^{d} and calculated as follows, for all fields except the precipitation field:

$$E^{\mathrm{d}} = sE + i. \tag{4}$$

For the global radiation and wind speed fields, when calculating the regression coefficients of the linear relationship, we force the intercept to 0 in order to avoid having possibly negative radiation or too flat a regression slope for wind speed.

For the precipitation field, we do not expect that the timing of precipitations in the ERA-I data set is accurate enough for the linear regression between F_{E} and E to be used as a way to de-bias E. Instead, we simply use the ratio of the sum of the elements of F_{E} over the sum of the elements of E, denoted as f. f is written as

$$f = \frac{\sum_{j=1}^{n_{\mathrm{E}}} F_{\mathrm{E},j}}{\sum_{j=1}^{n_{\mathrm{E}}} E_j}. \tag{5}$$

The de-biased precipitation field of the ERA-I data set, E^{d}, is then defined as $E^{\mathrm{d}} = fE$.

2.3.4 Reconstructing a diurnal cycle to the ERA-I data

In order to use the de-biased meteorological fields of the ERA-I data set to fill the gaps in the meteorological fields of the FLUXNET data set, they need to be interpolated from the original 3-hourly time step to the half-hourly time step.

For the instantaneous fields (all fields, except for the global radiation, the longwave radiation and the precipitation fields), the 3-hourly data are simply linearly interpolated in order to reconstruct a diurnal cycle at a half-hourly resolution. The half-hourly de-biased field of the ERA-I data set is denoted $E^{\mathrm{d}}_{\mathrm{F}}$ and is written as

Algorithm 3

for $j = 1 : n_{\mathrm{F}}$
{
$\quad l = ((j-1) r_{\mathrm{F}} - z)/r_{\mathrm{E}}$
$\quad E^{\mathrm{d}}_{\mathrm{F},j} = E^{\mathrm{d}}_{\mathrm{int}(l)} (\mathrm{mod}\,(l,1)) + E^{\mathrm{d}}_{\mathrm{int}(l+1)} (1 - \mathrm{mod}\,(l,1))$
} .

The global radiation field is distributed as a function of the solar angle, based on a code initially developed by J. C. Morrill within the frame of the GSWP (Global Soil Wetness Project; Dirmeyer, 2011) and used, for example, in the ORCHIDEE model (Krinner et al., 2005) (http://dods.ipsl.jussieu.fr/orchidee/DOXYGEN/webdoc/d1/db6/solar_8f90_source.html). The solar angle is a function of the longitude and latitude (long, lat), the day of the year (doy) and the hour (hour in UTC + 0). The solar angle is denoted α(long,lat,doy,hour); in the following, we will reduce this to α(hour).

For the global radiation, $E_{\mathrm{F}}^{\mathrm{d}}$ is defined as the corresponding E^{d} value, weighted by the ratio of the current solar angle to the mean solar angle over the 3-h time period (over which the E^{d} value is defined). $E_{\mathrm{F}}^{\mathrm{d}}$ is written as

Algorithm 4

$$
\begin{array}{l}
\text{for } j = 1 : n_{\mathrm{F}} \\
\{ \\
\quad l = ((j-1)r_{\mathrm{F}} - z)/r_{\mathrm{E}} \\
\quad \alpha_{\mathrm{cum}} = 0 \\
\quad \text{for } k = \mathrm{mod}\,(\mathrm{int}(l)r_E + r_F + z, 24) : \mathrm{mod}\,(\mathrm{int}(l+1)r_{\mathrm{E}} + z, 24) \\
\quad \{ \\
\qquad \alpha_{\mathrm{cum}} = \alpha\,(k) \\
\quad \} \\
\quad E_{\mathrm{F},j}^{\mathrm{d}} = \frac{\alpha(\mathrm{mod}(j r_{\mathrm{F}}, 24))}{\alpha_{\mathrm{cum}}} E_{\mathrm{int}(l+1)}^{\mathrm{d}} \\
\}\,.
\end{array}
$$

The incoming longwave radiation field is assumed to be uniformly distributed and consequently $E_{\mathrm{F}}^{\mathrm{d}}$ is written as

$$E_{\mathrm{F},j}^{\mathrm{d}} = E_{\mathrm{int}(l+1)}^{\mathrm{d}} \quad \text{for} \quad 1 \leq j \leq n_{\mathrm{F}} \tag{6}$$

For the precipitation field, a mean number of hours of precipitation (h) over a 3 h rainy period is calculated using the FLUXNET data set and used to distribute the precipitation. In this case, $E_{\mathrm{F}}^{\mathrm{d}}$ is written as

Algorithm 5

$$
\begin{array}{l}
\text{for } j = 1 : n_{\mathrm{F}} \\
\{ \\
\quad l = ((j-1)r_{\mathrm{F}} - z)/r_{\mathrm{E}} \\
\quad \text{if} \,\mathrm{mod}\,(l,1)\,\frac{r_{\mathrm{E}}}{r_{\mathrm{F}}} + 1 \leq \mathrm{round}\left(\frac{h}{r_{\mathrm{F}}}\right) \\
\quad \{ \\
\qquad E_{\mathrm{F},j}^{\mathrm{d}} = \frac{r_{\mathrm{E}}}{\mathrm{round}\left(\frac{h}{r_{\mathrm{F}}}\right) r_{\mathrm{F}}} E_{\mathrm{int}(l+1)}^{\mathrm{d}} \\
\quad \} \\
\quad \text{else } E_{\mathrm{F},j}^{\mathrm{d}} = 0 \\
\}\,.
\end{array}
$$

2.4 Statistics used for evaluating the gapfilling method

In order to evaluate the gapfilling method, we compare the E^{d} time series to the in situ time series F_{E} for each meteorological variable at each site. We also make use of the original ERA-I data set, E.

We use first the root mean square error (RMSE) and the standard deviation (SD) in two appropriate metrics in order to evaluate how the gapfilling method performs:

$$\mathrm{error\_reduction} = (1 - \mathrm{RMSE}(F_{\mathrm{E}}, E^{\mathrm{d}})/\mathrm{RMSE}(F_{\mathrm{E}}, E)) \times 100$$

$$\mathrm{relative\_error} = \mathrm{RMSE}(F_{\mathrm{E}}, E^{\mathrm{d}})/\mathrm{SD}(F_{\mathrm{E}}) \times 100.$$

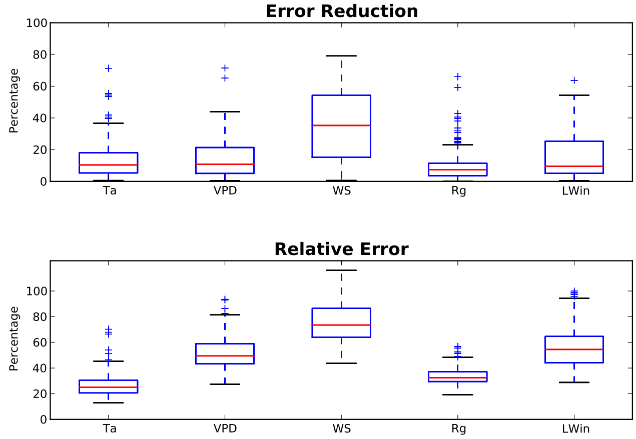

Figure 1. Distribution across sites of the error reduction (top panel) and relative error (bottom panel) of the bias correction method for air temperature, vapour pressure deficit, wind speed, global radiation and longwave incoming radiation. The box extends from the lower (25 %) to upper quartile (75 %) values of the data, with a red line at the median. The whiskers extend from the box to show the range of the data within 1.5 × (25–75 %) data range. Outliers are marked by crosses beyond the end of the whiskers.

The error reduction enables to know how the bias correction applied to the ERA-I data contributes to improving the fit to the in situ data. An error reduction of 50 % means that the bias correction cancels 50 % of the initial model–data mismatch. An error reduction of 0 % means that the ERA-I time series has no systematic error but only randomly distributed errors. The relative error shows how the root mean square error between the in situ data and the unbiased ERA-I data compares with the standard deviation of the in situ data. It helps to compare the error to the internal variability of the in situ data.

We also evaluate how the standard deviation of the ERA-Interim products before and after correction differs from the one of the FLUXNET data set by calculating normalized standard deviations ($\mathrm{SD}(E)/\mathrm{SD}(F_{\mathrm{E}})$ and $\mathrm{SD}(E^{\mathrm{d}})/\mathrm{SD}(F_{\mathrm{E}})$, respectively) in order to evaluate how much the data variability is maintained.

Lastly, we specifically evaluate the diurnal cycle interpolated from the 3-hourly de-biased meteorological fields of the ERA-I data set. To this end, two new time series have been constructed from F and $E_{\mathrm{F}}^{\mathrm{d}}$ by removing their daily mean values. The correlation between these two "anomaly" time series is calculated at each site, as is the standard deviation of the time series inferred from the ERA-I data set, normalized to the standard deviation of the one inferred from the FLUXNET data set.

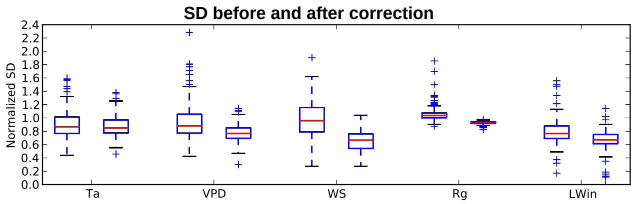

Figure 2. Distribution across sites of the normalized standard deviation of the ERA-I data before (left) and after (right) bias correction for air temperature, vapour pressure deficit, wind speed, global radiation and longwave incoming radiation. The box extends from the lower (25 %) to upper quartile (75 %) values of the data, with a red line at the median. The whiskers extend from the box to show the range of the data within 1.5 × (25–75 %) data range. Outliers are marked by crosses beyond the end of the whiskers.

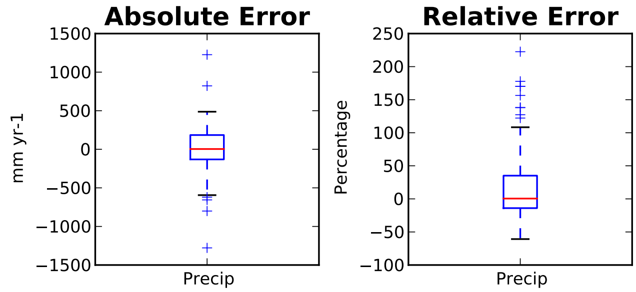

Figure 3. Distribution across sites of the error on the mean annual precipitation as measured at FLUXNET stations when using the ERA-I product, in absolute (mm yr^{-1}, left panel) and relative values (%, right panel). The box extends from the lower (25 %) to upper quartile (75 %) values of the data, with a red line at the median. The whiskers extend from the box to show the range of the data within the 1.5 × (25–75 %) data range. Outliers are marked by crosses beyond the end of the whiskers.

3 Results and discussion

3.1 De-biasing ERA-Interim time series

The mean error reduction for air temperature over all sites equals 14 % (Fig. 1). Scores vary significantly across sites. For most sites, the error reduction is less than 40 % (Fig. 1), showing that most of the mismatch between downscaled and measured data is due to non-systematic bias that our correction approach cannot account for. Sites for which the error reduction is higher than 40 % (IT-LMa, IT-Col, IT-Pia, ES-ES1, ES-ES2 and AT-Neu; Fig. 1) are mountain sites or located near the coast, locations where the meteorological local conditions (as recorded by the meteorological stations at FLUXNET sites) and meteorological conditions provided by ERA-Interim may vary the most.

The relative error varies across sites from low values (13 % for RU-Ha2 and CA-NS3) to up to 50 % or more (BW-Ghg, BW-Ghm, BR-Sa3, ID-Pag, US-Wi7). Sites where the relative error is low are located in continental regions where the air temperature varies significantly (by more than 40 °C) between the winter and summer period, leading to a very large standard deviation of the air temperature signal. Conversely, BR-Sa3 and ID-Pag are sites where the month-to-month variations in Ta are less than 4 °C. The two sites in Botswana have too few data (only in April 2003) to obtain a significant standard deviation of the air temperature signal. Indeed, US-Wi7 is the only site where the high relative error is due to a very high RMSE (5.4 °C after bias correction). This is probably due to a shift in the in situ air temperature timestamp, which leads to an important dephasing between FLUXNET and ERA-Interim time series on timescales shorter than a day.

The error reduction for the VPD (vapour pressure deficit) signal is of the same order as the one obtained for air temperature (mean value of 14 %, maximum of up to 60 %), but the relative error is much larger (mean value of 52 %), with only few sites having a relative error less than 40 %. The large relative error, which reflects the difficulty of correcting the ERA-Interim signal, might be partly due to the way we calculate VPD for ERA-Interim. It is inferred from the *dt2m* and *t2m* fields, which leads to the potential accumulation of the sources of errors from both of them.

Wind speed is the meteorological field for which the error reduction is the largest (mean value of 36 %). This large bias correction mainly reflects the fact that the reference heights at which the wind speed data are provided by ERA-interim (10 m) and measured at site level are different. Even though the error on wind speed is largely reduced, the remaining error after bias correction is still large, with a mean relative error over all sites of 76 % (minimum relative error is 40 % at NL-Haa, with an RMSE of less than 1 m s^{-1}).

The mean error reduction over all sites for global radiation equals 11 % (with only 21 sites having an error reduction higher than 20 %). The global radiation is the field for which the mean error reduction is the lowest. The highest error reductions are obtained for the sites US-Wi7 and US-Wi8, whose global radiation values appear abnormally low, especially when compared to nearby sites such as US-Wi4 or US-Wi5. This could be due to a problem in the units of the original data or in the data processing and correction before their publication in the La Thuile collection. The relative error after bias correction for global radiation (mean value of 34 %) is of the same order as the one obtained for air temperature (mean value of 27 %), but it varies much less across sites.

The longwave incoming radiation has a mean error reduction and relative error similar to the VPD field (17 and 57 %, respectively), with large site-to-site variations.

Figure 2 represents the normalized standard deviation (NSD) of the ERA-I products (Ta, VPD, WS, Rg and LWin) before and after the bias correction, and, consequently, it gives insights into how the de-biasing procedure impacts the internal variability of the meteorological fields (in comparison with the measured variability). Overall, the bias correction tends to reduce the spread of the NSD across sites. This is especially true for the global radiation field. The mean NSD is not significantly modified by the bias correction for air temperature (mean NSD before correction of 0.91 compared to 0.87 after correction) and global radiation (1.06 compared to 0.93). By contrast, the bias correction impacts negatively on the NSD of the vapour deficit (mean NSD of 0.94 vs. 0.77), the wind speed (mean NSD of 0.98 vs. 0.65) and the longwave incoming radiation (mean NSD of 0.80 vs. 0.64) from ERA-I. These negative impacts show the limits of a bias correction method based on linear regression for meteorological fields for which the bias between FLUXNET and ERA-I data do not vary linearly.

Regarding the precipitation field, for which we only correct for the cumulative flux over the observation period, the error reduction can be large, both in terms of absolute and relative values. Figure 3 and Table B1 show the distribution across sites of the error on the mean annual precipitation (MAP) field when using ERA-Interim precipitation fields, in absolute values ($\mathrm{mm\,yr^{-1}}$) and relatively to the MAP measured locally at FLUXNET sites (%). At BR-Sa3, the observed value equals $1250\,\mathrm{mm\,yr^{-1}}$ while the ERA-Interim precipitation field equals $2500\,\mathrm{mm\,yr^{-1}}$. Consequently, the error ($1250\,\mathrm{mm\,yr^{-1}}$) is as large as the observed value (relative error of 100 %). Similarly, there are other sites where ERA-Interim largely overestimates the observed value: the CA-NS1-7 sites (relative error no less than 78 %), SK-Tat (177 %) and US-SP1 (156 %). By contrast, there are other sites where ERA-Interim underestimates the observed values: AU-How (41 %), AU-Tum (53 %), AU-Wac (59 %) and CZ-BK1 (60 %). Interestingly, for many of these sites where model and data disagree the most, the climatological mean (CM, as reported on the FLUXNET website) is in better agreement with the mean annual precipitation as estimated by ERA-Interim than with that from the observations: BR-Sa3 ($\mathrm{CM} = 2043\,\mathrm{mm\,yr^{-1}}$), CA-NS1-7 ($\mathrm{CM} = 500\,\mathrm{mm\,yr^{-1}}$), CZ-BK1 ($\mathrm{CM} = 1025\,\mathrm{mm\,yr^{-1}}$) and US-SP1 ($\mathrm{CM} = 1310\,\mathrm{mm\,yr^{-1}}$). This is probably due to an underestimation of the precipitation measurements at the FLUXNET sites, where the WMO standard methodology to measure the precipitation is not always used. In addition the precipitation value measured at sites in cold environments does not always include snow precipitation, leading to underestimation of the total values. On average, over all sites, the mean relative error equals 34 % of the observed annual mean precipitation. When removing the 13 above-listed sites where model and data disagree the most, the relative error decreases to 24 %.

3.2 Reconstructing a diurnal cycle to the ERA-I data

We evaluate here how good the interpolation of the ERA-I data from original 3-hourly to half-hourly time steps is (Fig. 4).

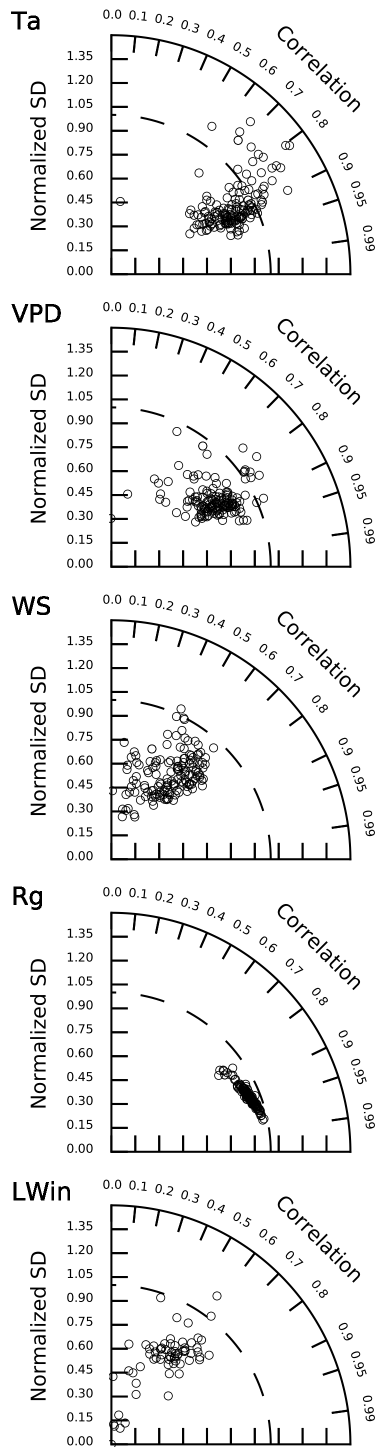

Figure 4. Taylor diagram representing the NSD and correlation (R) between the diurnal signals of the ERA-I and FLUXNET product for air temperature, vapour pressure deficit, wind speed, global radiation and longwave incoming radiation.

For air temperature, on average, over all sites, the mean correlation (R value) between the ERA-I and the FLUXNET time series equals 0.87, while the mean normalized standard deviation of the FLUXNET time series (NSD) equals 0.88. Across sites, there is a relative low spread of the correlation score, with few sites having a correlation lower than 0.8. NSD is more spread out, with values that range between 0.3 and 1.35.

For vapour pressure deficit, the model–data agreement in terms of diurnal cycle is lower that the one obtained for air temperature: mean R and NSD equal 0.72 and 0.69, respectively. The spread between sites, both in terms of R and NSD, is relatively reduced, but for most of the sites, the R and NSD values are close to the mean values.

Wind speed is the meteorological variable for which the diurnal cycle inferred from the ERA-I data set is least in agreement with the observation (mean R and NSD values of 0.47 and 0.69, respectively. The model performance varies greatly among sites, especially for the NSD that ranges between 0.3 and 1. This is particularly amplified by the correction factor we apply to the original ERA-I data set (s factor, Eq. 4). The s factor being at many sites lower than 1 tends to reduce the diurnal amplitude of the time series.

The diurnal cycle of the global radiation inferred from the ERA-I data set is in very good agreement with the observed one. None of the sites have values lower than 0.8 and 0.75 for R and NSD, respectively. For both R and NSD, the mean value over all sites equals 0.92.

The diurnal cycle for the incoming longwave radiation does not match the observed one, with mean values across sites of 0.51 and 0.64 for R and NSD, respectively. This score is comparable to the one obtained for wind speed. Note, however, that the diurnal cycle of these two variables is much less pronounced than the one of air temperature, global radiation and vapour pressure deficit. Consequently, it is more challenging to catch the diurnal cycle of these two variables.

4 Concluding remarks

4.1 Gapfilling of in situ data

The method presented in this study has shown its capacity for filling the gaps in meteorological data collected at FLUXNET sites. The performance of the method developed varies across sites and is also a function of the meteorological variable. The results, however, show that when large gaps are present, the proposed methodology is the best available strategy (when no nearby stations are present). Nevertheless, the performance of the method remains poor for the wind speed field, in particular regarding its capacity to conserve a standard deviation similar to the one measured at FLUXNET stations. A significant effort should be undertaken to improve the bias correction method that could in the future be based on a non-linear fit between the ERA-I and FLUXNET data set. In addition, some methodological issues remain, which are discussed below.

4.2 Checking for data quality

The method presented in this study is based on the assumption that the ERA-I data contain some biases that we can correct in order to better match local meteorological information at FLUXNET sites. Nevertheless, one may ask whether, for some specific variables at some sites, the diagnosed ERA-I vs. FLUXNET bias does not reveal a problem in the FLUXNET measurements rather than a bias within the ERA-I data. As presented in Sect. 3, this is possibly the case for, among others, the precipitation field for different sites, the global radiation (e.g. for site US-Wi8) and the air temperature (site US-Wi7). It is not our purpose to point out particular sites but rather to highlight that our method and the associated graphical tools may serve also to support data-quality controls.

4.3 Improving the FLUXNET data set for modelling purposes

As underlined in Sect. 1, the FLUXNET data set is highly valuable for modelling purposes in order to evaluate how terrestrial ecosystem models perform at site level. In order to get the most valuable information at site level, it would be of interest to add the atmospheric pressure field to the standard FLUXNET data sets. Even if atmospheric pressure slightly varies over time, this variable is a required input of many ecosystem models and it would be good to benefit from the data measured locally instead of using only data from reanalysis. Similarly, measurement and vegetation heights are key parameters for modelling the turbulent fluxes within and at the top of the canopy; these are not yet standardly available for all the sites in the FLUXNET data set. In our method, we bias-correct the wind speed at a height of 10 m of ERA-I to better match the observed values at site level, without knowing the height at which these observations have been collected. Using default values for vegetation and measurement heights may have strong limitations on some modelled energy fluxes (latent and sensible heat fluxes).

Appendix A

We provide here a numerical application of the main equations used in the pseudo-algorithms developed in this study for the first day of a data set for a site located in the time zone UTC + 2. The z parameter is consequently set to 2 (difference with respect to UTC), r_F equals 0.5 (resolution of FLUXNET meteorological data, half-hourly) and $r_E 3$ (3-hourly resolution of the ERA-Interim data).

Table A1. Numerical application of the main equations used in the pseudo-algorithms based on the records from the ERA-Interim data set.

No. of records: j	Corresponding timestamp for instantaneous variables (UTC + 0)	Corresponding time period for averaged variables (UTC + 0)	Alg. (1)	Alg. (2)	
			$(jr_E + z)/r_F$	$((j-1)r_E + z)/r_F + 1$	$(jr_E + z)/r_F$
1	03:00	00:00–03:00	12	7	12
2	06:00	03:00–06:00	18	13	18
3	09:00	06:00–09:00	24	19	24
4	12:00	09:00–12:00	30	25	30
5	15:00	12:00–15:00	36	31	36
6	18:00	15:00–18:00	42	37	42
7	21:00	18:00–21:00	48	43	48
8	00:00	21:00–00:00	54	49	54

Table A2. Numerical application of the main equations used in the pseudo-algorithms based on the records from the FLUXNET data set.

No. of records: j	Corresponding timestamp for instantaneous variables – local time	Corresponding timestamp for instantaneous variables – UTC + 0	Corresponding time period for instantaneous variables – local time	Corresponding time period for instantaneous variables – UTC + 0	[a]	int(l)	mod(l,1)	Alg. (4)			Alg. (5)	
								$\mathrm{mod}(\mathrm{int}(l)r_\mathrm{E}+r_\mathrm{F}+z, 24)$	$\mathrm{mod}(\mathrm{int}(l+1)r_\mathrm{E}+z, 24)$	$\mathrm{mod}(jr_\mathrm{F}, 24)$	$\mathrm{mod}(l,1)\frac{r_\mathrm{E}}{r_\mathrm{F}}+1$	$\mathrm{mod}(l,1)\frac{r_\mathrm{E}}{r_\mathrm{F}}+1 \leq \mathrm{round}\left(\frac{h}{r_\mathrm{F}}\right)$
1	00:30	22:30	00:00–00:30	22:00–22:30	−0.67	−1	0.50	23.5	2	0.5	3	1
2	01:00	23:00	00:30–01:00	22:30–23:00	−0.50	−1	0.67	23.5	2	1	4	0
3	01:30	23:30	01:00–01:30	23:00–23:30	−0.33	−1	0.83	23.5	2	1.5	5	0
4	02:00	00:00	01:30–02:00	23:30–00:00	−0.17	−1	0.00	23.5	2	2	6	0
5	02:30	00:30	02:00–02:30	00:00–00:30	0.00	0	0.17	2.5	5	2.5	1	1
6	03:00	01:00	02:30–03:00	00:30–01:00	0.17	0	0.33	2.5	5	3	2	1
7	03:30	01:30	03:00–03:30	01:00–01:30	0.33	0	0.50	2.5	5	3.5	3	1
8	04:00	02:00	03:30–04:00	01:30–02:00	0.50	0	0.67	2.5	5	4	4	0
9	04:30	02:30	04:00–04:30	02:00–02:30	0.67	0	0.83	2.5	5	4.5	5	0
10	05:00	03:00	04:30–05:00	02:30–03:00	0.83	0	0.00	2.5	5	5	6	0
11	05:30	03:30	05:00–05:30	03:00–03:30	1.00	1	0.17	5.5	8	5.5	1	1
12	06:00	04:00	05:30–06:00	03:30–04:00	1.17	1	0.33	5.5	8	6	2	1
13	06:30	04:30	06:00–06:30	04:00–04:30	1.33	1	0.50	5.5	8	6.5	3	1
14	07:00	05:00	06:30–07:00	04:30–05:00	1.50	1	0.67	5.5	8	7	4	0
15	07:30	05:30	07:00–07:30	05:00–05:30	1.67	1	0.83	5.5	8	7.5	5	0
16	08:00	06:00	07:30–08:00	05:30–06:00	1.83	1	0.00	5.5	8	8	6	0
17	08:30	06:30	08:00–08:30	06:00–06:30	2.00	2	0.17	8.5	11	8.5	1	1
18	09:00	07:00	08:30–09:00	06:30–07:00	2.17	2	0.33	8.5	11	9	2	1
19	09:30	07:30	09:00–09:30	07:00–07:30	2.33	2	0.50	8.5	11	9.5	3	1
20	10:00	08:00	09:30–10:00	07:30–08:00	2.50	2	0.67	8.5	11	10	4	0
21	10:30	08:30	10:00–10:30	08:00–08:30	2.67	2	0.83	8.5	11	10.5	5	0
22	11:00	09:00	10:30–11:00	08:30–09:00	2.83	2	0.00	8.5	11	11	6	0
23	11:30	09:30	11:00–11:30	09:00–09:30	3.00	3	0.17	11.5	14	11.5	1	1
24	12:00	10:00	11:30–12:00	09:30–10:00	3.17	3	0.33	11.5	14	12	2	1
25	12:30	10:30	12:00–12:30	10:00–10:30	3.33	3	0.50	11.5	14	12.5	3	1
26	13:00	11:00	12:30–13:00	10:30–11:00	3.50	3	0.67	11.5	14	13	4	0
27	13:30	11:30	13:00–13:30	11:00–11:30	3.67	3	0.83	11.5	14	13.5	5	0
28	14:00	12:00	13:30–14:00	11:30–12:00	3.83	3	0.00	11.5	14	14	6	0
29	14:30	12:30	14:00–14:30	12:00–12:30	4.00	4	0.17	14.5	17	14.5	1	1
30	15:00	13:00	14:30–15:00	12:30–13:00	4.17	4	0.33	14.5	17	15	2	1
31	15:30	13:30	15:00–15:30	13:00–13:30	4.33	4	0.50	14.5	17	15.5	3	1
32	16:00	14:00	15:30–16:00	13:30–14:00	4.50	4	0.67	14.5	17	16	4	0
33	16:30	14:30	16:00–16:30	14:00–14:30	4.67	4	0.83	14.5	17	16.5	5	0
34	17:00	15:00	16:30–17:00	14:30–15:00	4.83	4	0.00	14.5	17	17	6	0
35	17:30	15:30	17:00–17:30	15:00–15:30	5.00	5	0.17	17.5	20	17.5	1	1
36	18:00	16:00	17:30–18:00	15:30–16:00	5.17	5	0.33	17.5	20	18	2	1
37	18:30	16:30	18:00–18:30	16:00–16:30	5.33	5	0.50	17.5	20	18.5	3	1
38	19:00	17:00	18:30–19:00	16:30–17:00	5.50	5	0.67	17.5	20	19	4	0
39	19:30	17:30	19:00–19:30	17:00–17:30	5.67	5	0.83	17.5	20	19.5	5	0
40	20:00	18:00	19:30–20:00	17:30–18:00	5.83	5	0.00	17.5	20	20	6	0
41	20:30	18:30	20:00–20:30	18:00–18:30	6.00	6	0.17	20.5	23	20.5	1	1
42	21:00	19:00	20:30–21:00	18:30–19:00	6.17	6	0.33	20.5	23	21	2	1
43	21:30	19:30	21:00–21:30	19:00–19:30	6.33	6	0.50	20.5	23	21.5	3	1
44	22:00	20:00	21:30–22:00	19:30–20:00	6.50	6	0.67	20.5	23	22	4	0
45	22:30	20:30	22:00–22:30	20:00–20:30	6.67	6	0.83	20.5	23	22.5	5	0
46	23:00	21:00	22:30–23:00	20:30–21:00	6.83	6	0.00	20.5	23	23	6	0
47	23:30	21:30	23:00–23:30	21:00–21:30	7.00	7	0.17	23.5	2	23.5	1	1
48	00:00	22:00	23:30–00:00	21:30–22:00	7.17	7	0.00	23.5	2	0	2	1

[a] $l=((j-1)r_\mathrm{F}-z)\big/ r_\mathrm{E}$

Appendix B

Table B1. Error reduction (ER, %) and relative error (RE, %) of the bias correction method for air temperature (Ta), vapour pressure deficit (VPD), wind speed (WS), global radiation (Rg), longwave incoming radiation (LWin) and mean annual precipitation (mm yr^{-1}) as measured at FLUXNET stations (MAP_f) and as given by the ERA-I product (MAP_e).

Site	Ta		VPD		WS		Rg		LWin		Precip	
	ER	RE	ER	RE	ER	RE	ER	RE	ER	RE	MAP_f	MAP_e
AT-Neu	41.7	29.5	12.4	57.2	33.1	99.1	2.8	33.9	–	–	1401.6	1251.4
AU-Fog	8	42.9	33.3	54.9	15.4	94.1	0.3	28.7	54.4	40.5	1752	1424.4
AU-How	10.9	45.4	32.9	59	51.8	103.3	9.8	29.6	31.6	46.7	1927.2	1127
AU-Tum	24.1	44	25.9	58.7	0.7	109.2	5	29.9	–	–	1226.4	570.4
AU-Wac	12.2	46.5	26.9	65.1	4.7	84.5	31.9	55.4	–	–	1051.2	430.8
BE-Bra	5.2	22.7	4.4	44.6	46.6	62.7	15	32.6	–	–	876	858.8
BE-Jal	36.7	27.4	22	65	24.5	88.8	12.9	49	–	–	1401.6	928.2
BE-Lon	3.6	22.7	11.9	48.4	41.4	55.1	7.4	38.9	–	–	700.8	796.4
BE-Vie	30.9	20.2	5.7	48	69.1	60.6	10.2	35.6	–	–	876	850.5
BR-Sa3	19.2	66.4	–	–	–	–	0.3	37.6	7.3	69.3	1226.4	2452.8
BW-Ghg	14.3	54.2	5.2	69.9	–	–	5.1	38.7	24.2	98.7	–	–
BW-Ghm	6.6	51.2	11.6	74	–	–	6.3	36.8	19.5	97.4	–	–
BW-Ma1	1	32.2	3.9	49.6	26.6	84.3	0.5	23.5	14.6	57.6	350.4	648.9
CA-Man	1.3	14.7	9.6	46	0	73.1	16.7	32.5	–	–	350.4	604.1
CA-Mer	6.9	21.6	1.5	48.7	29.3	77.1	11.2	28.5	2.5	32.4	876	973.3
CA-NS1	36.5	13.1	17.8	38.4	38.5	65.8	2	29.3	–	–	175.2	473.5
CA-NS2	34.3	14.1	21.5	38.4	15.3	62.4	10.9	28.3	–	–	350.4	625.7
CA-NS3	8.4	13.4	0.6	38.7	50.4	58.8	4.2	28.1	–	–	175.2	565.2
CA-NS4	3.7	18.4	4	40.9	67.2	66	2.4	27.9	–	–	175.2	389.3
CA-NS5	1.7	15.3	0.5	38.2	65.1	62.9	3.3	28.3	–	–	175.2	398.2
CA-NS6	12.8	12.9	6.5	38	42.1	58.4	2.2	28.7	–	–	175.2	417.1
CA-NS7	11.6	13.8	9.5	37.2	73.4	67.8	4.1	29	–	–	350.4	661.1
CA-Qcu	8.9	13.7	0.5	41.9	14.3	57.3	10.6	31.7	2.9	37.6	876	962.6
CA-Qfo	8.8	13.1	2.8	38.2	51.6	59.4	7.9	29.2	1.2	35.7	876	941.9
CA-SF1	13.1	21.8	10.2	49.2	39.7	65.5	2.9	30	6.7	43.8	525.6	710.3
CA-SF2	11.3	23.7	0.8	50.3	50.6	71.1	3.4	29.9	3.1	43.6	350.4	625.7
CA-SF3	5.9	18.6	0.5	42.1	38.1	62.9	5.1	29.3	5.3	45.2	350.4	539.1
CH-Oe1	3.3	24.3	3.6	46.1	15.7	80.7	3.1	32.1	29.6	59	1226.4	1066.4
CH-Oe2	15.2	24.4	6.3	51.4	25.8	75.2	1.8	34.3	45.2	94.3	–	–
CZ-BK1	1	31.1	1.5	63.7	29.1	93.1	8.6	36.4	23.8	94.2	2102.4	824.5
CZ-wet	4.3	38.1	12.6	49.4	71	70.2	0	30.4	21.4	56.1	–	–
DE-Bay	28.1	26.9	10.3	50.3	31.4	85.1	10.2	36.2	–	–	1051.2	802.4
DE-Geb	10.4	20	4.8	40.1	16	57.1	4.9	29.3	1.8	52.5	525.6	710.3
DE-Gri	14.8	23.6	14.2	46.5	54.2	61.3	13.9	31.2	10.3	63.9	876	668.7
DE-Hai	8	24.7	7.4	47.2	33.1	74.8	5.5	31.3	5.8	45.9	700.8	620.2
DE-Kli	29.1	21.4	24.9	44.6	6.9	63.8	3.7	30.2	1.5	52.1	700.8	637.1
DE-Meh	0	18	1.2	38.2	24	55.6	5.9	30.2	2.9	48.9	525.6	665.3
DE-Tha	4.9	23.5	4.8	45.7	24.1	86.6	4.8	32.3	5.3	68.9	876	700.8
DE-Wet	26.5	28.7	16.6	51.2	4	90.1	8.3	33.3	4.9	52.5	1051.2	761.7
DK-Fou	8.1	20.7	0	43.5	43.7	67.2	6.7	31.2	–	–	700.8	737.7
DK-Lva	20.5	20.6	3.3	44.3	20.5	67.7	7.9	33.4	–	–	1051.2	796.4
DK-Ris	10.3	23.7	11.6	53.9	44.3	67.7	13.3	35.6	22.8	64.8	525.6	784.5
DK-Sor	17.2	24.8	4.9	61.4	57.1	60.6	13.3	35.9	1.3	64.7	876	639.4
ES-ES1	53.5	36.3	29.5	82.5	14.5	94.8	10.1	35.1	–	–	525.6	316.6
ES-ES2	54.4	35.5	24.2	80.2	3	88.6	6	33.5	45.6	56.7	700.8	317.1
ES-LMa	6.8	22.4	6.7	27.4	10.8	92.7	8.3	30.1	4.4	56.2	700.8	393.7
ES-VDA	21.6	45.4	22.4	81.4	1.6	95.9	1	42.5	3	64.5	1051.2	607.6
FI-Hyy	5.1	15.4	8	38.7	29.4	65.6	8.1	29.5	–	–	525.6	673.8
FI-Kaa	7	23.6	6	51.1	14.8	72.1	1	38.6	–	–	525.6	657
FI-Sod	4.5	22	0	47.5	8.9	73.8	2.7	41.3	–	–	350.4	547.5
FR-Fon	8.9	20.8	13	42.1	56.8	70.2	6.6	38.5	9.6	50.8	700.8	620.2
FR-Gri	0.6	20.1	0	41.7	48.9	58.6	5.2	37.5	23.4	45.6	525.6	657

Table B1. Continued.

Site	Ta		VPD		WS		Rg		LWin		Precip	
	ER	RE	ER	RE	ER	RE	ER	RE	ER	RE	MAP_f	MAP_e
FR-Hes	3.4	21.8	4	45.8	29.3	83.5	2.7	37.2	–	–	1051.2	922.1
FR-LBr	4.8	27.2	4.8	46.9	11.5	92.5	6.6	38.8	22.9	45.6	876	658.6
FR-Lq1	12.5	37.8	9.8	67.9	0	85.4	11.4	56.7	–	–	1051.2	991.7
FR-Lq2	12.5	37.8	9.8	67.9	0	85.4	11.4	56.7	–	–	1051.2	991.7
FR-Pue	18	25.5	5.3	45.9	37.2	84.9	4	38.8	7.5	44.6	876	700.8
HU-Bug	5.3	30.4	2.4	51.7	21.7	73	17.1	37.1	–	–	525.6	541.9
HU-Mat	3.6	24.1	9	47.4	40.2	100	7.3	37.4	–	–	525.6	500.6
ID-Pag	36.3	67.9	17.2	76.7	13.4	123.6	2.2	41.3	–	–	2102.4	1964.9
IE-Ca1	1.2	30.3	3.3	54.5	58.1	61.6	38.1	41.8	–	–	700.8	910.1
IE-Dri	36.2	27.8	12.6	62.3	62.8	64.8	20	37.6	7.2	56.7	1226.4	922.1
IL-Yat	13.8	38.4	15.2	55.8	2.8	78.8	0.9	19.9	36.7	64.2	350.4	278.1
IS-Gun	39.6	32.4	25	60.8	24.1	73.2	13.5	36.9	–	–	700.8	1187.8
IT-Amp	21.9	41.4	0	48.6	9	91	8.9	33.6	4.2	79.8	876	876
IT-BCi	31	28.4	19	69.8	3.9	94.2	9.5	26.5	31.4	60.1	1226.4	632.2
IT-Cas	11.7	26.5	27.5	50.7	57.3	97	3.6	25.1	52.7	54.5	876	818.7
IT-Col	55.4	35.2	35.3	65.8	16.7	88.5	17.4	36.3	32.1	65.5	1226.4	786.2
IT-Cpz	15.3	33.3	21.9	69.1	9.5	96.6	7.8	31.2	–	–	876	755.2
IT-Lav	13	36.2	11.3	76.9	12	106.2	0.2	36.6	5.3	56.4	876	1233.8
IT-Lec	12.9	22.3	39.3	40	–	–	3.5	33.7	–	–	350.4	493.5
IT-LMa	71.3	29.3	30.9	54.6	41.4	116.1	40.6	37.3	–	–	700.8	770.1
IT-Mal	35.3	39.5	39.1	93.6	0	110.8	9.9	38.8	–	–	1401.6	1523.5
IT-MBo	15.2	29.1	18.6	70.6	6.3	112.5	0.8	34.6	1.7	69.9	876	1307.5
IT-Non	9.6	24.7	3.4	42.6	38.2	103.7	3	41.1	–	–	876	818.7
IT-Pia	41.9	39.1	32.3	80.3	–	–	0.2	40	–	–	350.4	515.3
IT-PT1	30.3	23.7	32.7	48.8	33.3	97.8	2.1	32.5	–	–	876	748.7
IT-Ren	20.7	32.7	10.8	68	3.3	92.9	0.5	42.5	8	60.3	700.8	1112.4
IT-Ro1	36.4	25.6	1.6	43.3	7.9	79.1	3.8	26.7	21.4	79.3	876	826.4
IT-Ro2	33.1	25.9	12.1	44.3	34.1	80.2	1.8	27	–	–	876	803.7
IT-SRo	40.5	28.2	28.1	72.1	12.4	98.9	4.1	35.4	28.3	100	700.8	722.5
NL-Ca1	6.3	19.6	8	51.9	2.5	49	6.5	38	39.8	42	700.8	730
NL-Haa	7.8	23.7	–	–	20.8	43.6	13	30.4	–	–	876	730
NL-Hor	1.1	26.2	65.1	75.8	54.1	60.6	6.1	44.5	2.04	95.9	1051.2	756.3
NL-Lan	3.7	20.9	2.3	42.7	70	53	7.2	30.2	26.5	52	876	748.7
NL-Loo	8.1	17.9	11.2	40.6	65.9	60.3	10.3	31.6	32	49	876	730
NL-Lut	0.7	27.4	11.6	54.2	43.5	46.2	7.1	30.7	23.3	69.9	525.6	486.7
NL-Mol	5	16	1.8	39.4	75.6	57.9	6.3	30.2	63.7	59.7	525.6	510.3
PL-wet	6.4	25.8	5.9	41.5	54.8	63.9	4.8	30.9	16.2	56.4	525.6	491.2
PT-Esp	4.6	27.9	0.8	40.9	63.9	73.6	7.7	24.2	–	–	700.8	574.4
PT-Mi1	8.3	22.7	7.4	36.8	0.8	75.2	7.2	21.2	–	–	525.6	465.1
PT-Mi2	33.1	23.2	10.6	29.3	23.3	68.9	1.6	21.1	0.4	54.7	525.6	316.6
RU-Cok	8.2	34.6	26.9	86.4	0	63	0.2	44.2	16.9	97.6	175.2	473.5
RU-Fyo	5.2	15.4	0	42.6	70.6	76.5	1.8	30.7	5.2	43.7	525.6	772.9
RU-Ha1	18.7	16.1	13.7	42.6	0.6	73.2	7.9	33.8	–	–	525.6	710.3
RU-Ha2	17.6	13.3	15.6	43.4	2.8	81.9	10.4	32.9	–	–	–	–
RU-Ha3	20.7	23.8	15.3	45.4	9.1	100	2.6	32.7	–	–	–	–
RU-Zot	7.7	18.5	11.2	43.1	42.5	78.5	2.1	40.3	4.4	44.7	350.4	730
SE-Deg	3.6	28.4	0	46.3	28.1	66.2	10.2	31.9	–	–	525.6	720
SE-Faj	4.9	30.5	3.3	62.2	72.1	64.5	25.2	40.7	–	–	525.6	584
SE-Fla	6.8	22.2	8	44.6	11.1	69.8	25	31.3	–	–	700.8	865.2
SE-Nor	5.8	18.4	1.7	40.2	59.8	69.3	7.7	29.8	14.2	57.1	876	811.1
SE-Sk1	26.9	25.1	7.3	47.5	73.3	68.3	2.2	32	–	–	–	–
SE-Sk2	4.7	19.9	6.8	71.6	60.3	87.5	11.5	32.1	5.6	53.5	–	–
SK-Tat	1.2	34.2	15.6	69.5	–	–	16.1	33.5	–	–	175.2	486.7
UK-AMo	13.6	26.9	–	–	13.4	57	26.5	35.4	–	–	876	782.1

Table B1. Continued.

Site	Ta		VPD		WS		Rg		LWin		Precip	
	ER	RE	ER	RE	ER	RE	ER	RE	ER	RE	MAP_f	MAP_e
UK-EBu	1.8	32.7	4.7	55.8	–	–	10.8	41.4	–	–	1226.4	708.9
UK-ESa	5.7	25.8	10.5	54	67.7	60.1	6.5	38.7	–	–	350.4	547.5
UK-Gri	10.1	30.5	9.8	66.8	3.6	98.9	4.5	41.3	–	–	1051.2	1010.8
UK-Ham	8.7	23.9	44	60	75.1	52.3	3.1	32.1	–	–	700.8	604.1
UK-Her	28.4	29.5	8	38.4	65.3	63.9	8.4	26.5	–	–	700.8	667.4
UK-PL3	34.8	45.2	11.7	43	69.3	62.4	15.9	32.8	8.3	54.3	525.6	590.6
UK-Tad	10.7	25.9	–	–	47.3	66	9.5	32.8	–	–	525.6	740.3
US-ARM	9.2	18.7	8.8	39.3	22.8	82.2	11.4	28.1	40.2	80.6	700.8	560.6
US-Aud	5.7	28.7	10.7	41.8	2.3	72.6	2.4	23.8	44.1	37.7	350.4	302.1
US-Bar	1.8	20.1	0.4	47.5	48.7	84.9	1.8	31.8	–	–	1401.6	1401.6
US-Bkg	23.3	17.7	30	52.8	33.2	57.8	4.5	29.3	5.4	36.6	700.8	715.1
US-Blo	29.8	32.8	36.8	45.3	41.2	83.7	39.8	19.3	–	–	1226.4	734.4
US-Bo1	6.9	15.9	21.2	55.2	0	60.3	10.3	29.5	5.5	40.7	700.8	770.1
US-FPe	3.1	26.7	2.6	47.9	40.7	73.5	10	38.6	9.6	43	350.4	312.9
US-Goo	7	24.6	23.9	61.5	53.5	71.3	3.5	28.1	4.2	33.9	1576.8	1359.3
US-Ha1	16.7	20	25.1	56.9	47	73.4	33.7	29.8	–	–	1226.4	1264.3
US-Ho1	1.4	19	1.7	45.4	32.9	74.8	24.9	30.6	–	–	876	1200
US-Ho2	3.1	16.9	–	–	49.5	74.8	26.9	29.5	–	–	700.8	973.3
US-Los	9.8	27.6	–	–	34.2	69.5	4.4	30.8	–	–	700.8	796.4
US-Me4	2	33.1	12	37.6	36.3	94.6	12.9	32.4	–	–	525.6	938.6
US-MMS	3.3	22.3	22.9	58.6	8.7	85.5	8.2	28.8	17.7	29.9	1051.2	1020.6
US-MOz	13.1	18	15.3	48.3	30.3	65.9	4.2	27.1	5.4	28.8	876	755.2
US-Ne1	9.4	18.5	22.4	53.3	19.1	60.3	10.5	28.2	–	–	700.8	530.9
US-Ne2	13.3	18.9	26.2	54.1	27	62.2	7.4	28.1	–	–	700.8	480
US-Ne3	12.5	17.9	21.2	49.4	28.6	61.7	11.5	28.3	–	–	525.6	469.3
US-Oho	3.4	21.8	–	–	73.5	60.2	18.1	36	–	–	700.8	887.1
US-PFa	12.8	26.8	21.5	70.8	15	86.2	39.7	34.4	–	–	700.8	722.5
US-SP1	8	30.8	8.2	55.7	42.9	79.3	9.8	36.7	–	–	525.6	1347.7
US-SP2	15.8	37.5	1.5	58.9	41.7	83	7.1	33	–	–	1051.2	1181.1
US-SP3	13.8	33.5	5.1	57.3	48.5	84.4	10.9	33.4	–	–	1051.2	1251.4
US-SP4	17.8	27.2	25	53.3	58.2	70.2	30.8	28.6	–	–	1226.4	943.4
US-Syv	26.5	17.8	17.6	46.1	19.5	74.8	15.8	30.2	–	–	350.4	673.8
US-Ton	9.2	30.3	6.1	35.4	9.8	101.8	4.9	24.1	–	–	525.6	597.3
US-UMB	10.9	21.5	13.4	55.9	46.6	69.4	27.6	31.5	–	–	525.6	618.4
US-Var	3.1	26	11.7	29.6	54.7	91.9	4.6	25.7	–	–	525.6	604.1
US-WBW	12.1	23.6	–	–	16.4	92.7	1.4	29.3	–	–	–	–
US-WCr	3	17	32.4	70.3	55.9	69.6	10.7	30.5	17.1	33.3	700.8	707.9
US-Wi0	11.6	40.6	23.8	50.7	57	71.2	25.3	36.6	–	–	876	962.6
US-Wi1	8.2	29.6	7.6	59	72.1	78.3	42.7	52.7	–	–	175.2	417.1
US-Wi2	16.6	35.2	4.9	56.7	79.1	74.3	27.4	51.3	–	–	350.4	449.2
US-Wi4	9.8	24.8	9.7	52.3	60.8	74.3	22.5	48.3	–	–	700.8	700.8
US-Wi5	13	26.3	8.9	52.9	62.9	69.3	19.9	48.8	–	–	700.8	761.7
US-Wi6	13.8	28.3	14.5	50.1	42.3	71.7	24.3	36.9	–	–	876	931.9
US-Wi7	0.6	70.2	3.5	93.1	53.8	87.8	59.3	55.5	–	–	876	668.7
US-Wi8	11.4	23.9	14	50.7	77	80	66	36.2	–	–	1051.2	1106.5
US-Wi9	18.1	34	12.5	49.1	59	74	23	52.5	–	–	876	850.5
ZA-Kru	7.1	27.6	71.4	48.3	6.3	89.7	4.5	27.5	32.9	42	350.4	648.9

Acknowledgements. The authors sincerely thank the ECMWF for providing ERA-Interim reanalysis. The authors also thank Frédéric Chevallier, Fabienne Maignan and Nicolas Viovy for their help in using the ERA-Interim reanalysis data set. The authors thank the sites' PIs and staff for making the meteorological data used in this study available. These data were acquired by the FLUXNET community and in particular by the following networks: AmeriFlux (US Department of Energy, Biological and Environmental Research, Terrestrial Carbon Program (DE-FG02-04ER63917 and DE-FG02-04ER63911)), AfriFlux, AsiaFlux, CarboAfrica, CarboEuropeIP, CarboItaly, CarboMont, ChinaFlux, Fluxnet-Canada (supported by CFCAS, NSERC, BIOCAP, Environment Canada and NRCan), GreenGrass, KoFlux, LBA, NECC, OzFlux, TCOS-Siberia and USCCC. We acknowledge the financial support to the eddy covariance data harmonization provided by CarboEuropeIP, FAO-GTOS-TCO, iLEAPS, the Max Planck Institute for Biogeochemistry, National Science Foundation, the University of Tuscia, Université Laval, Environment Canada and the US Department of Energy and the database development and technical support from Berkeley Water Center, Lawrence Berkeley National Laboratory, Microsoft Research eScience, Oak Ridge National Laboratory, the University of California – Berkeley, and the University of Virginia. Dario Papale is grateful for support from the GeoCarbon EU project.

Edited by: G. König-Langlo

References

Adler, R. F, Huffman, G. J., Chang, A., Ferraro, R., Xie, P. P., Janowiak, J., Rudolf, B., Schneider, U., Curtis, S., Bolvin, D., Gruber, A., Susskind, J., Arkin, P., and Nelkin, E.: The Version-2 Global Precipitation Climatology Project (GPCP) Monthly Precipitation Analysis (1979–Present), J. Hydrometeor., 4, 1147–1167, 2003.

Anderson, D. E. and Verma, S. B.: Carbon-dioxide, water-vapor and sensible heat exchanges of a grain-sorghum canopy, Bound.-Lay. Meteorol., 34, 317–331, doi:10.1007/bf00120986, 1986.

Anderson, D. E., Verma, S. B., and Rosenberg, N. J.: Eddy-correlation measurements of CO2, Latent-heat, and sensible heat fluxes over a crop surface, Bound.-Lay. Meteorol., 29, 263–272, doi:10.1007/bf00119792, 1984.

Aubinet, M., Grelle, A., Ibrom, A., Rannik, U., Moncrieff, J., Foken, T., Kowalski, A. S., Martin, P. H., Berbigier, P., Bernhofer, C., Clement, R., Elbers, J., Granier, A., Grunwald, T., Morgenstern, K., Pilegaard, K., Rebmann, C., Snijders, W., Valentini, R., and Vesala, T.: Estimates of the annual net carbon and water exchange of forests: The EUROFLUX methodology, Adv. Ecol. Res., 30, 113–175, 2000.

Baldocchi, D. D.: Assessing the eddy covariance technique for evaluating carbon dioxide exchange rates of ecosystems: past, present and future, Global Change Biol., 9, 479–492, doi:10.1046/j.1365-2486.2003.00629.x, 2003.

Baldocchi, D., Falge, E., Gu, L. H., Olson, R., Hollinger, D., Running, S., Anthoni, P., Bernhofer, C., Davis, K., Evans, R., Fuentes, J., Goldstein, A., Katul, G., Law, B., Lee, X. H., Malhi, Y., Meyers, T., Munger, W., Oechel, W., Paw U, K.T., Pilegaard, K., Schmid, H. P., Valentini, R., Verma, S., Vesala, T., Wilson, K., and Wofsy, S.: FLUXNET: A new tool to study the temporal and spatial variability of ecosystem-scale carbon dioxide, water vapor, and energy flux densities, B. Am. Meteorol. Soc., 82, 2415–2434, doi:10.1175/1520-0477(2001)082<2415:fantts>2.3.co;2, 2001.

Balsamo, G., Albergel, C., Beljaars, A., Boussetta, S., Brun, E., Cloke, H., Dee, D., Dutra, E., Muñoz-Sabater, J., Pappenberger, F., de Rosnay, P., Stockdale, T., and Vitart, F.: ERA-Interim/Land: a global land surface reanalysis data set, Hydrol. Earth Syst. Sci., 19, 389–407, doi:10.5194/hess-19-389-2015, 2015.

Balzarolo, M., Boussetta, S., Balsamo, G., Beljaars, A., Maignan, F., Calvet, J.-C., Lafont, S., Barbu, A., Poulter, B., Chevallier, F., Szczypta, C., and Papale, D.: Evaluating the potential of large-scale simulations to predict carbon fluxes of terrestrial ecosystems over a European Eddy Covariance network, Biogeosciences, 11, 2661–2678, doi:10.5194/bg-11-2661-2014, 2014.

Beer, C., Reichstein, M., Tomelleri, E., Ciais, P., Jung, M., Carvalhais, N., Roedenbeck, C., Arain, M. A., Baldocchi, D., Bonan, G. B., Bondeau, A., Cescatti, A., Lasslop, G., Lindroth, A., Lomas, M., Luyssaert, S., Margolis, H., Oleson, K. W., Roupsard, O., Veenendaal, E., Viovy, N., Williams, C., Woodward, F. I., and Papale, D.: Terrestrial Gross Carbon Dioxide Uptake: Global Distribution and Covariation with Climate, Science, 329, 834–838, doi:10.1126/science.1184984, 2010.

Blyth, E., Gash, J., Lloyd, A., Pryor, M., Weedon, G. P., and Shuttleworth, J.: Evaluating the JULES Land Surface Model Energy Fluxes Using FLUXNET Data, J. Hydrometeorol., 11, 509–519, doi:10.1175/2009jhm1183.1, 2010.

Boussetta, S., Balsamo, G., Beljaars, A., Panareda, A.-A., Calvet, J.-C., Jacobs, C., van den Hurk, B., Viterbo, P., Lafont, S., Dutra, E., Jarlan, L., Balzarolo, M., Papale, D., and van der Werf, G.: Natural land carbon dioxide exchanges in the ECMWF integrated forecasting system: Implementation and offline validation, J. Geophys. Res.-Atmos., 118, 5923–5946, doi:10.1002/jgrd.50488, 2013.

Dee, D. P., Uppala, S. M., Simmons, A. J., Berrisford, P., Poli, P., Kobayashi, S., Andrae, U., Balmaseda, M. A., Balsamo, G., Bauer, P., Bechtold, P., Beljaars, A. C. M., van de Berg, L., Bidlot, J., Bormann, N., Delsol, C., Dragani, R., Fuentes, M., Geer, A. J., Haimberger, L., Healy, S. B., Hersbach, H., Holm, E. V., Isaksen, L., Kallberg, P., Koehler, M., Matricardi, M., McNally, A. P., Monge-Sanz, B. M., Morcrette, J. J., Park, B. K., Peubey, C., de Rosnay, P., Tavolato, C., Thepaut, J. N., and Vitart, F.: The ERA-Interim reanalysis: configuration and performance of the data assimilation system, Q. J. Roy. Meteorol. Soc., 137, 553–597, doi:10.1002/qj.828, 2011.

Desjardins, R. L. and Lemon, E. R.: Limitations of an eddy-correlation technique for the determination of the carbon dioxide and sensible heat fluxes, Bound.-Lay. Meteorol., 5, 475–488, doi:10.1007/bf00123493, 1974.

Desjardins, R. L., Buckley, D. J., and Stamour, G.: Eddy flux measurements of CO_2 above corn using a microcomputer system, Agric. Forest Meteorol., 32, 257–265, doi:10.1016/0168-1923(84)90053-4, 1984.

Dirmeyer, P. A.: A History and Review of the Global Soil Wetness Project (GSWP), J. Hydrometeorol., 12, 729–749, doi:10.1175/jhm-d-10-05010.1, 2011.

Foken, T.: The energy balance closure problem: An overview, Ecol. Appl., 18, 1351–1367, doi:10.1890/06-0922.1, 2008.

Jung, M., Reichstein, M., Ciais, P., Seneviratne, S. I., Sheffield, J., Goulden, M. L., Bonan, G., Cescatti, A., Chen, J., de Jeu, R., Dolman, A. J., Eugster, W., Gerten, D., Gianelle, D., Gobron, N., Heinke, J., Kimball, J., Law, B. E., Montagnani, L., Mu, Q., Mueller, B., Oleson, K., Papale, D., Richardson, A. D., Roupsard, O., Running, S., Tomelleri, E., Viovy, N., Weber, U., Williams, C., Wood, E., Zaehle, S., and Zhang, K.: Recent decline in the global land evapotranspiration trend due to limited moisture supply, Nature, 467, 951–954, doi:10.1038/nature09396, 2010.

Kim, J., Yu, G., and Miyata, A.: AsiaFlux-sustaining ecosystems and people through resilience thinking, in: WCC-3 – Climate Sense, edited by: World Meteorological Organization,, p. 165–168, Tudor Rose, Leicester, UK, 2009.

Krinner, G., Viovy, N., de Noblet-Ducoudre, N., Ogee, J., Polcher, J., Friedlingstein, P., Ciais, P., Sitch, S., and Prentice, I. C.: A dynamic global vegetation model for studies of the coupled atmosphere-biosphere system, Global Biogeochem. Cycles, 19, GB1015, doi:10.1029/2003gb002199, 2005.

Mahecha, M. D., Reichstein, M., Carvalhais, N., Lasslop, G., Lange, H., Seneviratne, S. I., Vargas, R., Ammann, C., Arain, M. A., Cescatti, A., Janssens, I. A., Migliavacca, M., Montagnani, L., and Richardson, A. D.: Global Convergence in the Temperature Sensitivity of Respiration at Ecosystem Level, Science, 329, 838–840, doi:10.1126/science.1189587, 2010.

Murray, F. W.: On the computation of saturation vapor pressure, J. Appl. Meteorol., 6, 203–204, 1967.

Ohtaki, E.: Application of an infrared carbon-dioxide and humidity instrument to studies of turbulent transport, Bound.-Lay. Meteorol., 29, 85–107, doi:10.1007/bf00119121, 1984.

Papale, D.: Data Gap Filling, edited by: Aubinet, M., Vesala, T., and Papale, D., Eddy Covariance, A Practical Guide to Measurement and Data Analysis, Springer Atmospheric Sciences, 159–172, 2012.

Running, S. W., Baldocchi, D. D., Turner, D. P., Gower, S. T., Bakwin, P. S., and Hibbard, K. A.: A global terrestrial monitoring network integrating tower fluxes, flask sampling, ecosystem modeling and EOS satellite data, Remote Sens. Environ., 70, 108–127, doi:10.1016/s0034-4257(99)00061-9, 1999.

Stöckli, R., Lawrence, D. M., Niu, G. Y., Oleson, K. W., Thornton, P. E., Yang, Z. L., Bonan, G. B., Denning, A. S., and Running, S. W.: Use of FLUXNET in the community land model development, J. Geophys. Res.-Biogeosciences, 113, G01025, doi:10.1029/2007jg000562, 2008.

Stoy, P. C., Richardson, A. D., Baldocchi, D. D., Katul, G. G., Stanovick, J., Mahecha, M. D., Reichstein, M., Detto, M., Law, B. E., Wohlfahrt, G., Arriga, N., Campos, J., McCaughey, J. H., Montagnani, L., Paw U, K. T., Sevanto, S., and Williams, M.: Biosphere-atmosphere exchange of CO_2 in relation to climate: a cross-biome analysis across multiple time scales, Biogeosciences, 6, 2297–2312, doi:10.5194/bg-6-2297-2009, 2009.

Teuling, A. J., Seneviratne, S. I., Stoeckli, R., Reichstein, M., Moors, E., Ciais, P., Luyssaert, S., van den Hurk, B., Ammann, C., Bernhofer, C., Dellwik, E., Gianelle, D., Gielen, B., Gruenwald, T., Klumpp, K., Montagnani, L., Moureaux, C., Sottocornola, M., and Wohlfahrt, G.: Contrasting response of European forest and grassland energy exchange to heatwaves, Nature Geoscience, 3, 722–727, doi:10.1038/ngeo950, 2010.

Valentini, R., Matteucci, G., Dolman, A. J., Schulze, E. D., Rebmann, C., Moors, E. J., Granier, A., Gross, P., Jensen, N. O., Pilegaard, K., Lindroth, A., Grelle, A., Bernhofer, C., Grunwald, T., Aubinet, M., Ceulemans, R., Kowalski, A. S., Vesala, T., Rannik, U., Berbigier, P., Loustau, D., Guomundsson, J., Thorgeirsson, H., Ibrom, A., Morgenstern, K., Clement, R., Moncrieff, J., Montagnani, L., Minerbi, S., and Jarvis, P. G.: Respiration as the main determinant of carbon balance in European forests, Nature, 404, 861–865, doi:10.1038/35009084, 2000.

Zhao, Y., Ciais, P., Peylin, P., Viovy, N., Longdoz, B., Bonnefond, J. M., Rambal, S., Klumpp, K., Olioso, A., Cellier, P., Maignan, F., Eglin, T., and Calvet, J. C.: How errors on meteorological variables impact simulated ecosystem fluxes: a case study for six French sites, Biogeosciences, 9, 2537–2564, doi:10.5194/bg-9-2537-2012, 2012.